Exploring the Oscillatory Dynamics of a Forbidden Returns Inventory System

Xun Wang [a,*], Stephen M. Disney [b], Jing Wang [a]

[a] *School of Economics and Management, BeiHang University, Beijing, 100191, China.*

[b] *Logistics Systems Dynamics Group, Cardiff Business School, Cardiff University, Colum Drive, Cardiff, CF10 3EU, UK.*

Abstract

We present an analytical investigation of the intrinsic oscillations in a nonlinear inventory system where excessive inventory cannot be returned to the supplier. Mathematically this is captured by a non-negative constraint on the replenishment order. By studying the eigenvalues of the characteristic matrices of the system, the criteria for different types of dynamic behaviour (including convergence, periodicity, quasi-periodicity, chaos, and divergence) are derived. The upper and lower bounds of the order and inventory oscillations are found via a time-domain analysis. Our results are verified by bifurcation diagrams. We find that the closer the replenishment rule feedback parameters are to the convergence area, the milder the intrinsic oscillation of the system.

Keywords: Nonlinear inventory system; forbidden returns; oscillation, bifurcation, stability.

1. Introduction and motivation

A supply chain's inventory control policy needs to attenuate fluctuations in demand, so as to maintain a smooth production rate in the face of both externally and internally generated disturbances. It should also maintain inventory levels around target safety stock levels. One of the most well-studied oscillation phenomena in supply chains is the so-called Bullwhip Effect. Since the pioneering work of Lee *et al.* (1997), much effort has been devoted to this problem. Many factors affecting the Bullwhip Effect have been investigated including: the impact of forecasting methods (Chen *et al.*, 2000; Dejonckheere *et al.*, 2003); statistical modelling of demand processes (Aviv, 2003, Gaalman, 2006); cooperative mechanisms such as information sharing (Lee *et al.*, 2000; Dejonckheere *et al.*, 2004); and Vendor Managed Inventory (Disney and Towill, 2003a). The integration of control theory and system dynamics approaches provides a powerful approach for quantifying and mitigating such effect (Disney and Towill., 2003b). However, in most of the previous theoretical studies on the Bullwhip Effect, linear inventory system models were adopted. In linear systems dynamical oscillations can only be generated by external events (such as demand). This has greatly limited the applicability of published results and has made it impossible to explain and describe oscillations caused by internal factors.

To maintain linearity of inventory system models, order rates are permitted to take negative values. This means that all participants in a supply chain are allowed to return excess product freely. Specifically, a negative order rate value leads to a decrease in the inventory level at the consuming echelon and an immediate increase in the inventory level at the supplying echelon. This assumption may be difficult to realize in reality but we do recognize that it exists in some supply chains. For example in the consumer electronics and book publishing supply chains it is accepted practice that retailers may return unwanted product to the manufacturer / publisher. In practice this may also mean that the excess inventory is not physically moved from one location to another but instead will be considered to be in the possession of the upstream supplier until being used as part of a future

[*] Corresponding author. Tel.: +86 10 8233 8930.
E-mail: paul.wong.buaa@gmail.com (X. Wang), DisneySM@cardiff.ac.uk (S.M. Disney), pekwjing@public.bta.net.cn (J. Wang).

replenishment (Hosoda and Disney, 2009).

It has also been demonstrated that nonlinear effects play an important role in inventory systems, sometimes even a dominant role (Nagatani and Helbing, 2004). When linearity assumptions are removed complex dynamic behaviours are revealed. The behaviour may even become chaotic or hyper-chaotic. More importantly, oscillations generated internally by the system itself, rather than by the external environment, may arise. Mosekilde and Larsen (1988) adapted the beer game model (Sterman, 1989) to include both forbidden returns and lost sales constraints. To make the chaotic phenomenon more obvious, a long lead-time was used. Mosekilde and Larsen (1988) found that the operating cost of this constrained system could be 500 times higher than its linear counterpart. Thomsen *et al.* (1992) concluded that economic and business systems do not necessarily operate close to their steady state. Hwarng and Xie (2008) investigated several system factors that affect chaotic behaviour and discovered a 'chaos-amplification' phenomenon between supply chain echelons. Wu and Zhang (2007), using a supply chain model with a constrained discount rate and exponential demand function, found that the attractors of the model in the phase space moves with the assumed initial states, rendering it impossible to provide guidelines for avoiding chaos by bifurcation analysis. Wang *et al.* (2005) used the Lyapunov exponent to identify chaotic demand in real supply chain data and proposed an algorithm to cope with it from a time series aspect.

The piecewise linear modelling approach has also been shown to be effective for certain nonlinear supply chain problems as the piecewise linear function is able to approximate any nonlinear function to any required level of accuracy. Liu (2005) and Rodrigues and Boukas (2006) analyzed the stability of supply chain inventory systems with piecewise linear techniques. Laugesen and Mosekilde (2006) and Mosekilde and Laugesen (2007) studied border-collision bifurcations in piecewise linear supply chain systems. However, mathematical properties of such systems, such as local and global stability conditions and bifurcations, are still "very hard to investigate" and "notoriously challenging" (Sun, 2010).

This paper is concerned with identifying the range of oscillations in a constrained supply chain that are generated by the system itself rather than by the external environment. For our analysis a unit step demand input will be adopted (unless otherwise stated) to emphasize that it is the system itself rather than the environment that is generating these dynamical effects. The pattern and amplitude of each kind of oscillation will be characterized. Section 2 models the constrained one echelon supply chain system piecewise-linearly. Section 3 investigates the type of oscillation pattern produced by the inventory system. Section 4 focuses on the upper and lower bounds of oscillation with respect to the order volume and inventory level. Concluding remarks are given in Section 5.

2. Modelling and assumptions of forbidden returns inventory system

Our inventory system model has several components that can be described in the time domain by difference equations. These equations will be listed below. First, we assume that the inventory system uses exponential smoothing as a forecasting method. The exponential smoothing forecasts are generated with

$$\hat{d}_t = \alpha_F d_t + (1-\alpha_F)\hat{d}_{t-1}, \tag{1}$$

where d_t is the demand at time *t*, $\hat{d}_t$ is its forecast at time *t* and α_F is the exponential smoothing constant. $0 \le \alpha_F < 2$ is required for stability of the forecasting system. Within the inventory system, the inventory levels obey the usual conservation law such that the new level of inventory equals the inventory level in the previous period plus the net in-flow into that state. That is

$$i_t = i_{t-1} + c_t - d_t, \tag{2}$$

Here i_t is the inventory level, c_t is the completion rate (what arrives from the supplier or the production system) and o_t is the order rate at time. Factors such as the loss / damage / late delivery of goods in storage and transportation will be omitted. The work-in-progress, WIP, (or orders placed but not yet received) also obeys the conservation law,

$$w_t = w_{t-1} + o_{t-1} - c_t = \sum_{i=1}^{T_p} o_{t-i}, \tag{3}$$

where w_t is the work-in-process level and T_p is the physical lead-time. To capture the time delay between placing an order and receiving it into inventory there is a sequence of events delay for (information) order processing of one period and a physical lead-time, T_p, for production / transportation, also of one period duration. This means that

$$r_t = o_{t-1}, \tag{4}$$

and

$$c_t = r_{t-1}. \tag{5}$$

r_t is an auxiliary variable used to capture the review period and ensure a proper sequence of events. This assistant variable is also essential in establishing the matrix form of the inventory system. We make this unit lead-time assumption for the simplicity in future analysis. Non-negative WIP is assured as the orders cannot be negative; this fact is most easily recognized from the RHS of (3). It is clear from existing research on linear inventory system analysis that increasing the lead-time will severely harm the dynamic performance and reduce the size of its stability region in the parametrical space, Towill and Disney (2008). We note that it is theoretically possible to extend this analysis to higher lead-time cases. However the complexity of the analysis increases with the lead-time and, as we will demonstrate, this system already exhibits a very rich set of dynamics behaviours, even with such a short, known and constant lead-time.

Using these four building blocks (the forecast, the inventory and WIP balance equations and the lead-time equations), we adopt the Automatic Pipeline and Variable Inventory and Order Based Production Control System (APVIOBPCS) ordering policy for placing replenishment orders. For a thorough review of this policy and the entire IOBPCS family we refer readers to Sarimveis *et al.* (2008). This policy has been frequently studied as it is of a very general nature. This policy determines the replenishment order quantity as the sum "the demand forecast, plus a fraction of inventory discrepancy, plus a fraction of work-in-process discrepancy" (Disney and Towill, 2003a). The APVIOBPCS replenishment rule is a generalization of the industrially popular Order-Up-To policy, Dejonckheere et al (2003), and has a long history in the literature. Inventory and work-in-process discrepancies are the expected levels, $\hat{i}_t$ and $\hat{w}_t$, minus the actual levels, i_t and w_t, respectively. In the APVIOBPCS model, expected inventory level is set as a multiple k of expected demand (k is a constant called "target inventory gain"). The expected work-in-process is a multiple T_p of expected demand, $\hat{w}_t = T_p \hat{d}_t$ (Sarimveis *et al.*, 2008). For simplicity we set $k = 1$ and $T_p = 1$. Therefore $\hat{i}_t = \hat{w}_t = \hat{d}_t$. We use α_S and α_{SL} to denote the fractions arbitrarily set by decision makers. The subscript S is for stock (inventory), SL for supply line (work-in-process). In other words, α_S and α_{SL} are proportional feedback controllers acting upon the of inventory and work-in-process information used to generate a replenishment order. The APVIOBPCS ordering policy can be expressed as

$$\begin{aligned} o_t &= \left[\hat{d}_t + \alpha_S (\hat{i}_t - i_t) + \alpha_{SL} (\hat{w}_t - w_t) \right]^+ \\ &= \left[\hat{d}_t + \alpha_S (\hat{d}_t - i_t) + \alpha_{SL} (\hat{d}_t - w_t) \right]^+ \\ &= \left[(1 + \alpha_S + \alpha_{SL}) \hat{d}_t - \alpha_S i_t - \alpha_{SL} w_t \right]^+ . \end{aligned} \tag{6}$$

The ordering policy in (6) was found to mimic real-life decisions made by players of the Beer Game, Sterman (1989). Forbidden returns (non-negative orders) are enforced with the maximum operator, $[x]^+ = \max[0, x]$, in (6). Contrary to the linear assumption, we assume that when the desired order rate (calculated by the expression inside the square bracket in (6)) is negative, the supply chain participant can only stop ordering and wait for the excess inventory to be depleted before positive orders are resumed. Since there is no non-negative constraint on the inventory level, the following underlying assumptions are necessary: express orders / outsourcing are fully available (downstream demand can still be fulfilled even if supplier's inventory is insufficient); and shortages (backorders) are allowed. That is, negative inventory can be accumulated into the next period (Hosoda and Disney, 2012). Whilst we recognize that in real situations non-negative inventory is an important practical consideration, we have ignored this feature here so as to avoid the extra complexity and to isolate and specifically investigate the impact of non-negative orders.

We can see that the forecast is used three times to create the replenishment order. The first forecast is a forecast of the demand in the period after the lead-time. The second forecast is used to set target inventory levels. The third forecast is used to forecast the target open orders placed but not yet received the target WIP. We note when there is a unit step increase in demand that the orders will initially overshoot the demand in order to maintain inventory levels around target levels. After some time, when operating in a stable mode, the orders will "lock" onto the demand. Because of the lead-time between placing an order and receiving it into stock, this fundamental property of a replenishment system cannot be avoided if inventory levels are to be adequately maintained around target safety stock levels. This can be easily verified via a simulation analysis.

The above difference equations are easily converted into matrices that describe the system of equations that define the replenishment policy:

$$\mathbf{A}_1 = \begin{bmatrix} 1-\alpha_F & 0 & 0 & 0 & 0 \\ (1-\alpha_F)(1+\alpha_S+\alpha_{SL}) & -\alpha_{SL} & -\alpha_S & -\alpha_{SL} & \alpha_{SL}-\alpha_S \\ 0 & 0 & 1 & 0 & 1 \\ 0 & 1 & 0 & 1 & -1 \\ 0 & 1 & 0 & 0 & 0 \end{bmatrix}, \quad \mathbf{b}_1 = \begin{bmatrix} \alpha_F \\ \alpha_S+\alpha_F(1+\alpha_S+\alpha_{SL}) \\ -1 \\ 0 \\ 0 \end{bmatrix},$$

$$\mathbf{A}_2 = \begin{bmatrix} 1-\alpha_F & 0 & 0 & 0 & 0 \\ 0 & 0 & 0 & 0 & 0 \\ 0 & 0 & 1 & 0 & 1 \\ 0 & 1 & 0 & 1 & -1 \\ 0 & 1 & 0 & 0 & 0 \end{bmatrix}, \quad \mathbf{b}_2 = \begin{bmatrix} \alpha_F \\ 0 \\ -1 \\ 0 \\ 0 \end{bmatrix}, \quad \mathbf{x} = \begin{bmatrix} \hat{d} & o & i & w & r \end{bmatrix}^T. \tag{7}$$

The piecewise affine model for this nonlinear inventory system is given by

$$\mathbf{x}_t = \begin{cases} F_1(\mathbf{x}_{t-1}) = \mathbf{A}_1\mathbf{x}_{t-1} + \mathbf{b}_1 d_t, & \mathbf{x}_{t-1} \in S_1 \\ F_2(\mathbf{x}_{t-1}) = \mathbf{A}_2\mathbf{x}_{t-1} + \mathbf{b}_2 d_t, & \mathbf{x}_{t-1} \in S_2 \end{cases} \tag{8}$$

where $S_1 = \{\mathbf{x} \mid o \geq 0\}$ and $S_2 = \{\mathbf{x} \mid o < 0\}$ are both non-degenerate polyhedral partitions of the state space. That is, each region S_i is a (convex) polyhedron with a non-empty interior. The (n–1) dimensional hyper-plane $o_t = 0$ is the boundary of the partitions. $S_1 \cup S_2 = \mathrm{R}^n$, $S_1^\circ \cap S_2 = S_1 \cap S_2^\circ = \varnothing$. S° is the interior of S and n is the dimension of $\mathbf{x}$. It should be noted that the boundaries are continuous, i.e., $\mathbf{A}_1\mathbf{x}_t = \mathbf{A}_2\mathbf{x}_t$ when $\mathbf{x}_t \in S_1 \cap S_2$.

In general terms, the feedback parameters, α_S and α_{SL}, and the lead-time solely determine the stability of the inventory system. They also influence other dynamic characteristics of the system (Disney, 2008) The forecast is a feed-forward component in the inventory system that does not directly influence the stability of the inventory system. As long as $0 < \alpha_F < 2$, the forecasting system is stable and the stability of the inventory system is not influenced by the forecast. We now set the demand forecast to be equal to the deterministic demand (that is set $\alpha_F = 1$). As we mainly study the deterministic unit step demand, this assumption is not wildly unrealistic. Furthermore we are interested in the long term (not the initial transient response) dynamic behaviour. In the long term the exponential smoothing forecast has "locked" onto the step demand. Setting $\hat{d}_t = d_t$ does not alter the long-term behaviour of the inventory system and allows us to focus solely on the influence of α_S and α_{SL} in our discussion. Setting $\hat{d}_t = d_t$ also results in a naïve forecasting strategy, often advocated by the lean production community as a practical way to set production targets (Martichenko and von Grabe, 2010).

Our model can be further simplified. When the transportation lead time is one, the work-in-process is a flow rate rather than a stock level, i.e., $r_t = w_t$. If we let $r_t = w_t$ and $\alpha_F = 1$, we can express the inventory system in three dimensions with the following matrices:

$$\mathbf{A}_1 = \begin{pmatrix} -\alpha_{SL} & -\alpha_S & -\alpha_S \\ 0 & 1 & 1 \\ 1 & 0 & 0 \end{pmatrix},\ \mathbf{b}_1 = \begin{pmatrix} 1+2\alpha_S+\alpha_{SL} \\ -1 \\ 0 \end{pmatrix},\ \mathbf{A}_2 = \begin{pmatrix} 0 & 0 & 0 \\ 0 & 1 & 1 \\ 1 & 0 & 0 \end{pmatrix},\ \mathbf{b}_2 = \begin{pmatrix} 0 \\ -1 \\ 0 \end{pmatrix},\ \mathbf{x} = \begin{pmatrix} o \\ i \\ w \end{pmatrix}.$$

Noticing that $\mathbf{A}_1$ and $\mathbf{A}_2$ are both linear dependent, the dimension of the system can be further reduced. Denoting the sum of the inventory and work-in-process as the inventory position, that is $IP_t = i_t + w_t$, we have

$$\mathbf{A}_1 = \begin{pmatrix} -\alpha_{SL} & -\alpha_S \\ 1 & 1 \end{pmatrix},\ \mathbf{b}_1 = \begin{pmatrix} 1+2\alpha_S+\alpha_{SL} \\ -1 \end{pmatrix},\ \mathbf{A}_2 = \begin{pmatrix} 0 & 0 \\ 1 & 1 \end{pmatrix},\ \mathbf{b}_2 = \begin{pmatrix} 0 \\ -1 \end{pmatrix},\ \mathbf{x} = \begin{pmatrix} o \\ IP \end{pmatrix}. \tag{9}$$

Introducing the inventory position IP_t into the model is mathematically prudent as then a redundant dimension can be eliminated and both $\mathbf{A}_1$ and $\mathbf{A}_2$ become fully ranked. The use of IP_t does not alter the dynamics of the system in anyway. The steady-state behaviour of the original five-dimension model is exactly the same as the two-dimension system as long as the exponential smoothing forecasting mechanism is stable.

3. Pattern of oscillation in the forbidden returns system

The oscillation of linear systems is easy to investigate compared to nonlinear systems. There are only two patterns of dynamic behaviours that are physically possible. The system could be convergent (stable), which means that the trajectory will eventually return to an equilibrium point, no matter where it is started. That is, it is insensitive to initial values. It could also be divergent (unstable), which means the trajectory will escape to infinity. There is also a third pattern, appearing when the control parameters are on the very edge of the stability boundary called critical stability. Here the system will oscillate with a regular, repeating pattern.

On the other hand, trajectories of nonlinear systems could be either convergent or divergent and can even oscillate in a bounded fashion. It could oscillate in a regular repeating pattern or in a seemingly random one. The dynamic behaviour of the system could also be highly sensitive to initial values. Moreover, in piecewise linear systems, the effect of border-collisions can be dominant. This phenomenon refers when two linear systems are "sewn" together and where one of the part of the periodic trajectory becomes tangent to the sewing surface. This causes a particular type of bifurcation, named as border-collision bifurcation or C bifurcation in Russian literature (di Bernardo et al., 1999). In our forbidden returns inventory system, a border collision indicates that the inventory has grown large but negative orders cannot be issued. A simple type of border collision bifurcation consists of the continuous transformation of a solution from one type into another or the merging and disappearances of solutions of different types. However, more complicated nonlinear phenomena, including chaos, are possible (Zhusubaliyev and Mosekilde, 2003). Some examples of the different types of time domain oscillations in response to a unit step input are shown in Figure 1, where we asserted that convergent responses result in the lowest supply chain cost, divergent responses high supply chain cost. This assertion is based solely on intuition.

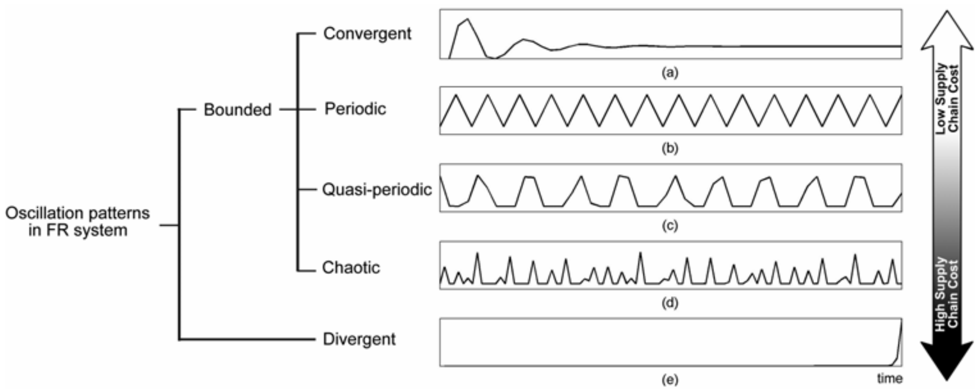

Figure 1: Five groups of dynamic behaviours (to the unit step demand) generated by the forbidden returns system

Figure 2 shows divergent (white), convergent (black) and periodic (dark grey) areas of the inventory system on the $\{\alpha_S,\ \alpha_{SL}\}$ plane. The matrices used to derive the criteria are also labelled. Quasi-periodicity and chaos are represented by light grey. We will explain in this section how to derive the boundaries analytically for each region. We have extended our scope from the conventional region when $0 \le \{\alpha_S, \alpha_{SL}\} \le 1$ to the case where an uninformed and irrational replenishment rule design exists because parameters are chosen outside of the stability region.

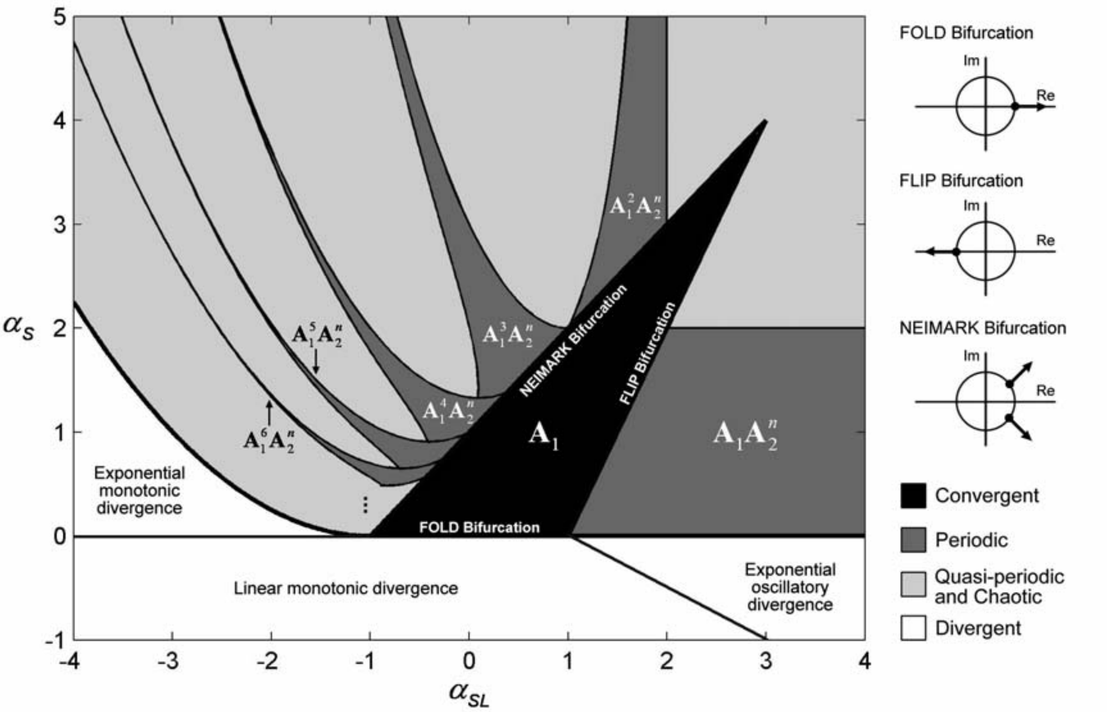

Figure 2. Bifurcation structure of forbidden returns inventory system.

3.1 Boundedness and divergence

If all solutions of a dynamical system that start out near an equilibrium point $\mathbf{x}_e$, stay near $\mathbf{x}_e$ forever, then the system is bounded (Figure 1a-d). Otherwise the system is divergent (Figure 1e). There are two factors in the forbidden returns system that cause three types of divergence in this system: exponential monotonic; linear monotonic; and exponential oscillatory divergence. Sometimes the sub-system F_1 dominates which will create an exponential (multiplicative) monotonic divergence. At other times the sub-system F_2 dominates which will create a linear (additive) divergence. Sometimes these two effects may combine and lead to an exponential and oscillating divergence.

The criteria for exponential monotonic divergence in the piecewise linear system is $\text{im}(\boldsymbol{\lambda}_{\mathbf{A}_1}) = 0$ and $\boldsymbol{\lambda}_{\mathbf{A}_1} > 1$, where im($z$) is the imaginary part of the complex number z. This is different from linear systems where the criteria for divergence is simply $\left|\boldsymbol{\lambda}_{\mathbf{A}_1}\right| = 1$. In linear systems, if the eigenvalues of system matrices are complex and outside the unit circle, the system oscillates with ever increasing amplitude, i.e., infinity becomes a focus of the system. However, in the piecewise linear forbidden returns systems, such trajectory will eventually hit the border at o_t = 0. In other words, the border constrains such trajectories from divergence. For exponential divergence to occur, infinity must be a node and the trajectories must not collide with the border, i.e., $\mathbf{A}_1$ has two real positive eigenvalues larger than one. Thus, the criterion for bounded oscillation is given by

$$\alpha_S = (\alpha_{SL} + 1)^2 / 4. \tag{10}$$

It is also worth noticing that this region and the asymptotic stability region are not adjacent. The second type of divergence (linear monotonic) happens when the parameters cross the saddle-node (fold) bifurcation boundary at $\alpha_S = 0$. If the parameters cross this boundary, the system will have only one positive eigenvalue larger than one, and the system trajectories starting from the origin will move along the negative axis of o_t linearly to infinity, under the effect of the linear sub-system F_2. Managerially, this means the firm never places orders even when inventory backlogs are accumulating. If $\alpha_S < -(\alpha_{SL} - 1)/2$, it will diverge linearly. Otherwise an exponential oscillatory divergence can be observed.

3.2 Convergence

If all solutions that start near $\mathbf{x}_e$ converge to $\mathbf{x}_e$, then more strongly, the system is convergent. This means that the trajectory approaches an equilibrium point over time (Figure 1a). The concept is mathematically equivalent to *asymptotic stability*, and has a similar meaning with *stability* in a classical linear control theory sense. In the area of convergence on the parametrical plane, the system will eventually return to equilibrium. The condition for stability is $\left|\boldsymbol{\lambda}_{\mathbf{A}_1}\right| < 1$. For $\mathrm{im}(\lambda_{\mathbf{A}_1}) = 0$ and $\lambda_{\mathbf{A}_1} = 1$, we have $\alpha_S = 0$, which is the criteria for saddle-node (fold) bifurcation. For $\mathrm{im}(\lambda_{\mathbf{A}_1}) = 0$ and $\lambda_{\mathbf{A}_1} = -1$, we have $\alpha_S = 2\alpha_{SL} - 2$, which is the criteria for period-doubling (flip) bifurcation. For $\mathrm{im}(\lambda_{\mathbf{A}_1}) \neq 0$ and $\left|\lambda_{\mathbf{A}_1}\right| = 1$, we have $\alpha_S = \alpha_{SL} + 1$. This is the criteria for Neimark bifurcation (Thompson and Stewart, 1986). These three criteria form a triangular stability region on the parametrical plane. In this region the system has a globally stable fixed point at {o = 1, ip = 1}. A similar pattern has been found in a two-dimensional discrete nonlinear system with saturation (Galias and Ogorzalek, 1990). The three types of bifurcation are labelled in Figure 2.

3.3 Periodicity

The *periodicity* of a system is a point which the system returns to after a certain number of function iterations or a certain amount of time (see Figure 1b for an illustration). In a forbidden returns system, conditions of periodic oscillations can be obtained by studying the eigenvalues of the corresponding matrix representing the periodic movement. That is to say, for a stable period-m movement under certain parameter settings, the modulus of eigenvalues of matrix $\mathbf{A}_1^{m-1}\mathbf{A}_2^n$ must be less than one, $\{m,n\} \in \mathbb{Z}^+$. We notice that the value of n does not affect the eigenvalues of matrix $\mathbf{A}_1^m\mathbf{A}_2^n$ (note $n > 0$) since the two dimensional matrix $\mathbf{A}_2$ is idempotent.

As an example, the conditions for a stable period-2 orbit can be derived by solving $\left|\boldsymbol{\lambda}_{\mathbf{A}_1\mathbf{A}_2}\right| < 1$, from which we obtain $0 < \alpha_S < 2$. Likewise, the criteria for period-3, $S_1^2 S_2^n$ can be obtained from $\boldsymbol{\lambda}_{\mathbf{A}_1^2\mathbf{A}_2} = 1$, i.e., $\left|\alpha_S\alpha_{SL} - 2\alpha_S + 1\right| = 1$, from which we get $\alpha_{SL} = 2$ and $\alpha_S = \dfrac{2}{2-\alpha_{SL}}$.

For a specific value of m, we can use this approach to derive the criteria for m + 1 periodicity. These regions form what is called an "Arnold's Tongue" in Figure 2 (Ogorzalek and Galias, 1991). The principal zone of period-2 lies on the right of the stability triangle. Other resonant zones are situated above the Neimark bifurcation boundary. We are unable to illustrate all the zones since there is an infinite number of them. But it is possible to infer that, as the period increases, they will finally approach the exponential divergence boundary, where the density of tongues will be very high.

3.4 Quasi-periodicity and chaos

Quasi-periodicity is a form of irregular motion that arises through the beating of two or more oscillatory modes with incommensurate frequencies (see Figure 1c). This form of dynamics can be observed in linear as well as in nonlinear systems. Quasi-periodic behaviour is also distinguished from deterministic chaos by not displaying sensitivity to the initial conditions. Geometrically, quasi-periodicity indicates that every trajectory winds around endlessly on a torus, never intersecting itself and yet never quite closing.

Mathematically, chaos refers to a very specific kind of unpredictability: deterministic behaviour that is very sensitive to its initial conditions. In other words, infinitesimal variations in initial conditions for a chaotic dynamic system lead to large variations in behaviour over time. Chaotic systems consequently appear disordered and random (Figure 1d). When chaotic dynamics occurs, the system moves in a region of phase space that is *densely* filled with unstable periodic orbits. The trajectory is attracted and repelled in different directions by these orbits, resulting in an irregular behaviour that is sensitive to small perturbations and parameter changes (Thompson and Stewart, 1986). In the forbidden returns system, quasi-periodic and chaotic oscillations are both characterized by the fact that, although bounded in phase space, the trajectory never precisely repeats itself.

To verify our analytical result, we conducted a numerical analysis which scans the parametrical plane. To distinguish periodicity, we adopted the numerical method proposed by Dai and Han (2011) which involves calculating the so-called Periodicity Ratio. Boundedness and asymptotic stability can be identified by calculating the variance of system response. In the bounded oscillation region, if the system is neither asymptotically stable nor periodic, then it must be quasi-periodic or chaotic. The accuracy of the numerical analysis is restricted by the thresholds that we arbitrarily set. In total 800×800 scans are carried out within the parameter place defined by $\alpha_S \in (-1,5)$ and $\alpha_{SL} \in (-4,4)$. In each scan, the first 100 data points are discarded and the next 2000 iterations are used to characterize the dynamic response. We use black for asymptotic stability, dark grey for periodicity, light grey for quasi-periodicity and chaos, and white for divergence. By comparing Figure 2 and Figure 3, we see that our analysis successfully explains the system behaviour. Figure 4 shows in more detail the structure of periodicity region when $\alpha_S \in (0.05, 0.1)$ and $\alpha_{SL} \in (-1.05, -1)$. We can easily notice the existence of a very delicate pattern called "sausage structure" (Ogorzalek and Galias, 1991) or "necklace structure" (Mosekilde and Laugesen, 2007) and has apparently an infinite number of successive patterns with a stable periodic movement.

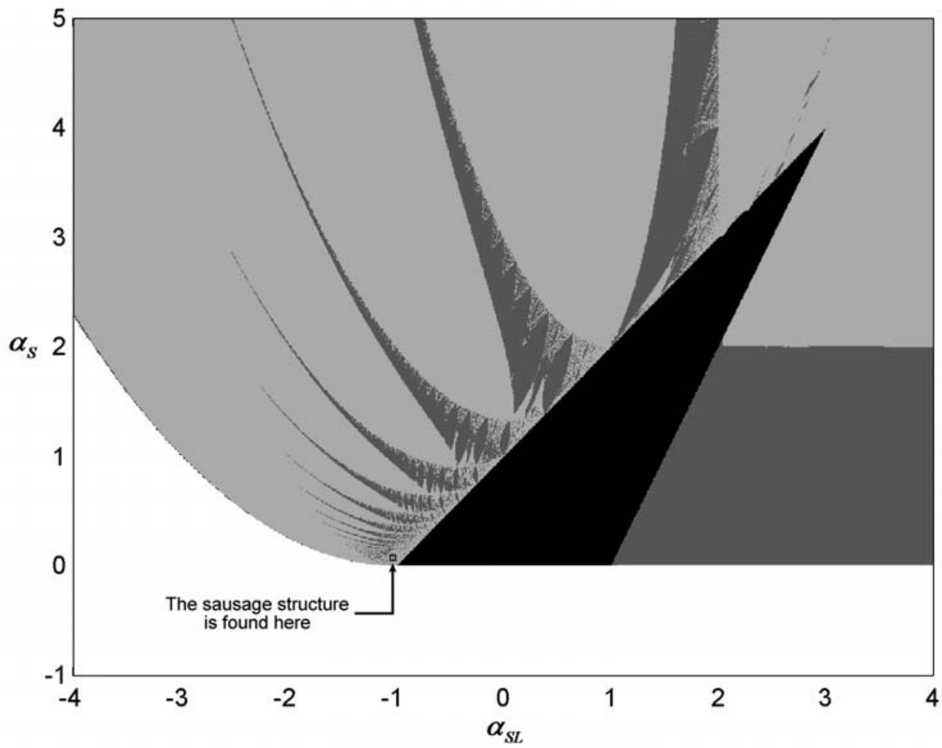

Figure 3. Numerical validation of the oscillation patterns in the forbidden returns system

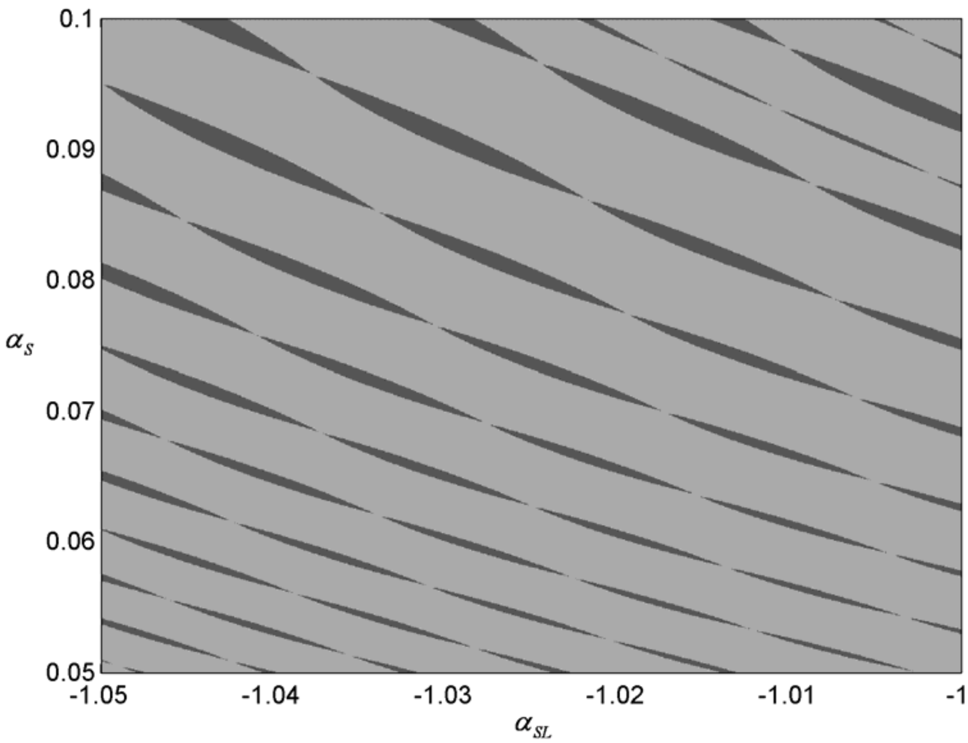

Figure 4. The "sausage" or "necklace" structure

To summarize, the aforementioned criteria divided the parametrical plane into several areas in which the inventory system oscillates in different patterns: convergent, periodic, quasi-periodic, chaotic and divergent. As intuition would dictate, a positive inventory feedback parameter is essential to maintain boundedness of the system. Furthermore, when the absolute value of α_{SL} is small, the system will be convergent. This region is limited and shaped as a triangle. Luckily the Order-Up-To policy ($\alpha_S = 1$, $\alpha_{SL} = 1$) lies within this region. Comparing these results with Laugesen and Mosekilde (2006), we see that for an inventory system which has a delivery time of two periods, asymptotic stability of a conservative ordering policy ($\alpha_S \in (0,1)$, $\alpha_{SL} \in (0,1)$) is assured. However, as the lead-time increases, an ordering policy with high inventory compensation and low WIP compensation (α_S close to 1 and α_{SL} close to 0) cannot guarantee the stability of the inventory system in this region. Also, positive inventory or work-in-process feedback (negative α_S or α_{SL}) will cause divergence (which can either be exponential or linear). Regular periodicity can be discovered when α_S is small and α_{SL} is positively large. Other areas are filled by periodical tongues, quasi-periodic and chaotic parameter settings. What we can infer from the above analysis is that high α_S and α_{SL} values can lead to chaos in nonlinear systems.

4. Bound of oscillation in the forbidden returns system

So far we have obtained the conditions for asymptotic stability, boundedness and stable periodicity in forbidden return systems. We are now interested in the bounds of oscillation because it is relevant to the variance amplification phenomenon in supply chains known as the Bullwhip Effect, which may severely increase the cost of operating supply chains (Geary et al., 2006). Figure 5 shows the result of a numerical analysis where the demand is a stochastic, independently and identically normally distributed with a mean of 10 and a standard deviation of unity, $d \sim N(10,1)$. $\alpha_S = 1$ and α_{SL} ranges from -1 to 3 with an increment of 0.04. The dashed line represents the bullwhip in a linear inventory system; the empty circles represent bullwhip in a corresponding forbidden returns system; and filled circles represent bullwhip also in the forbidden returns system, but with a deterministic step input ($d_t = 10$ for $t > 0$, $d_t = 0$ otherwise). Bullwhip is measured by the variance of the orders.

First we discover the bullwhip of the forbidden returns system will not inflate to infinity when the parameters approach or cross the stable boundary, which is obviously a consequence of non-negative orders. Second, linear bullwhip expressions no longer approximate bullwhip in the forbidden return system even in the centre of the stable region – the border collisions reduce the order variance. Third, knowledge of system oscillation in a deterministic environment is able to broadly predict bullwhip behaviour of the nonlinear system faced with stochastic demand, especially outside the stable region. Therefore a useful, meaningful and tractable first step is to calculate upper and lower bounds of system oscillation in the absence of randomness via the unit step response.

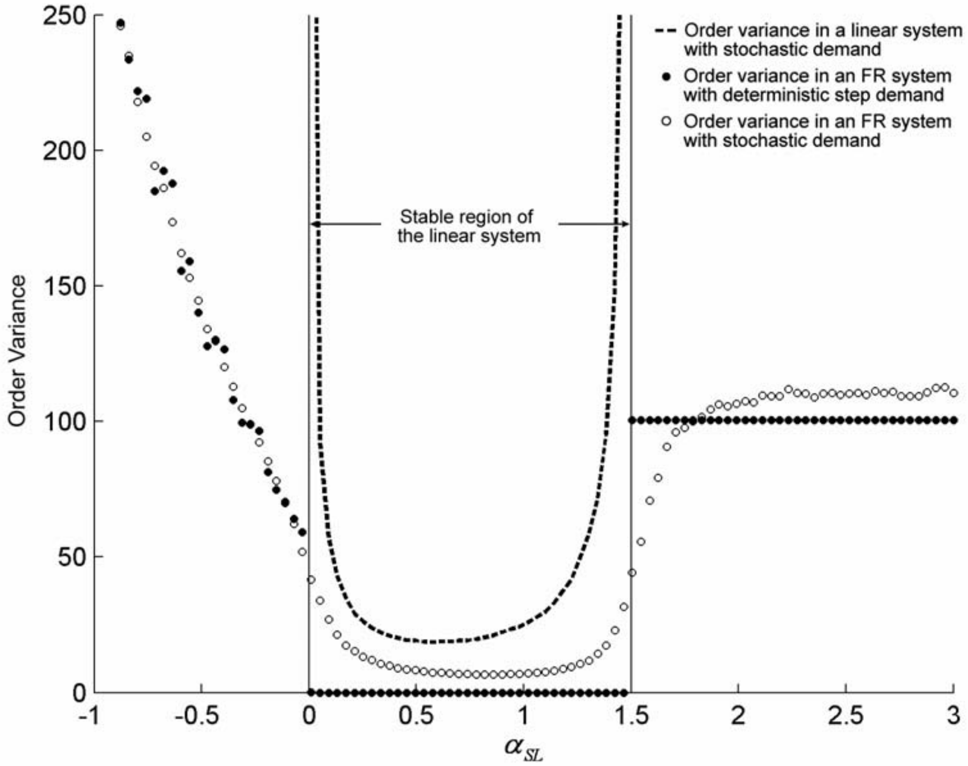

Figure 5. Comparison of the Bullwhip curve in linear and forbidden return systems

Recall that the piecewise inventory system model (8) contains a primary subsystem F_1 and a constrained subsystem F_2. Using the transformation $TF(q) = (q\mathbf{I} - \mathbf{A}_1)^{-1}\mathbf{b}_1$ we can derive the transfer function between the state variables (more specifically the order rate) and the input variable (the demand rate). **I** is the identity matrix with the appropriate dimension.

$$\frac{o(q^{-1})}{d(q^{-1})} = \frac{(1+2\alpha_S + a_{SL})q^{-1} - (1+\alpha_S + \alpha_{SL})q^{-2}}{1+(\alpha_{SL}-1)q^{-1} + (\alpha_S - \alpha_{SL})q^{-2}}, \tag{11}$$

where q^{-1} is the unit time lag operator (Åström, 1970). We may rewrite (11) into the following time domain form,

$$o_t + (\alpha_{SL}-1)o_{t-1} + (\alpha_S - \alpha_{SL})o_{t-2} = (1+2\alpha_S + \alpha_{SL})d_{t-1} - (1+\alpha_S+\alpha_{SL})d_{t-2}.$$

In the following analysis the assumption of unit step demand is once again adopted. Note that it is different from the numerical analysis in the beginning of this section where are assumed the demand was *i.i.d.*, $N(10,1)$. Because $d_t \equiv 1$ for $t > 0$ we can find the following second order recursive equation for order rate dominates the dynamics of the system:

$$o_t = (1-\alpha_{SL})o_{t-1} + (\alpha_{SL} - \alpha_S)o_{t-2} + \alpha_S. \tag{12}$$

It is worth noting that the coefficients in (12) equals $\mathrm{tr}(\mathbf{A}_1)$ and $-|\mathbf{A}_1|$ respectively. The layout of the eigenvalues of the system in the $\{\alpha_S, \alpha_{SL}\}$ plane is summarized in Figure 6. It is found that this layout and more precisely, the sign of the eigenvalues' real parts, determines the upper bounds of the orders.

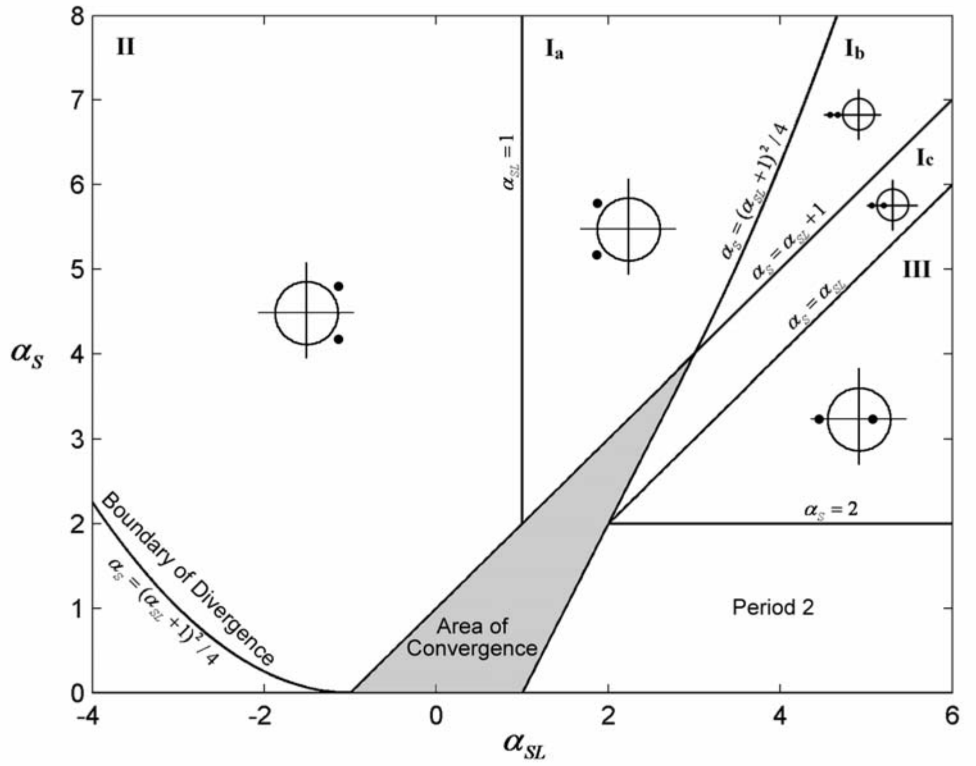

Figure 6. Eigenvalue layout in the $\{\alpha_{SL}\text{-}\alpha_S\}$ plane

4.1 Oscillations in the replenishment orders

A period-2 oscillation happens when α_S is small ($0 < \alpha_S < 2$) and α_{SL} is large ($\alpha_{SL} > 2 + \alpha_S / 2$). To analyze the oscillation in this region, we have to solve the following matrix equation $\mathbf{A}_1(\mathbf{A}_2\mathbf{x}+\mathbf{b}_2)+\mathbf{b}_1 = \mathbf{x}$ since the movement S_1S_2 dominates. By doing so we can get the oscillation of order: … 2, 0, 2, 0, 2, 0, … where the initial transient response of the system is omitted. In this region the oscillation is independent of α_S and α_{SL}, and the frequency of the order being zero is exactly 0.5.

In regions I_a, I_b and I_c in Figure 6, both of the eigenvalues have negative real parts. The boundaries for region I are $\alpha_{SL} = 1$ and $\alpha_S = \alpha_{SL}$. Therefore we have the following proposition:

Proposition 1. If $\{\alpha_S,\alpha_{SL}\}$ lies in region I, then $o_t \le \alpha_S$.

Proof. In region I we have $1-\alpha_{SL} \le 0$ and $\alpha_{SL} - \alpha_S \le 0$, which are coefficients of o_{t-1} and o_{t-2} in (12). Since all orders are non-negative it is easy to obtain $o_t \le \alpha_S$. □

In region II the system has two complex conjugate eigenvalues with positive real parts. To derive the expression for the upper bounds of the orders in this region the following transformation needs to be introduced. Starting from $t = 3$ and the basic difference equation (12), we make certain transformations to reach the form,

$$o_t = P_t^{(2)} o_2 + P_t^{(1)} o_1 + P_t^{(0)} , \tag{13}$$

$t \in \mathbb{N}^+$. $P_t^{(2)}$, $P_t^{(1)}$ and $P_t^{(0)}$ are different time varying coefficients. Bracketed superscripts should not be mistaken for multiple derivatives. The following proposition holds for the upper bound of the orders in this region:

Proposition 2. If $\{\alpha_S,\alpha_{SL}\}$ lies within region II, and $P_t^{(2)} < 0$, $P_{t-1}^{(2)} > 0$, then $o_t \le P_t^{(0)}$.

Proof. For coefficients $P_t^{(0)}$, $P_t^{(1)}$ and $P_t^{(2)}$, we have the following recursive relationships:

$$P_t^{(2)} = (1-\alpha_{SL})P_{t-1}^{(2)} + (\alpha_{SL} - \alpha_S)P_{t-2}^{(2)}; \tag{14}$$

$$P_t^{(1)} = (1-\alpha_{SL})P_{t-1}^{(1)} + (\alpha_{SL} - \alpha_S)P_{t-2}^{(1)}; \tag{15}$$

$$P_t^{(0)} = (1-\alpha_{SL})P_{t-1}^{(0)} + (\alpha_{SL} - \alpha_S)P_{t-2}^{(0)} + \alpha_S; \tag{16}$$

$$P_t^{(1)} = (\alpha_{SL} - \alpha_S)P_{t-1}^{(2)}. \tag{17}$$

Proof of (14) to (16) is elementary. (17) can be proved by induction. Notice $P_3^{(2)} = 1-\alpha_{SL}$, $P_4^{(1)} = (1-\alpha_{SL})(\alpha_{SL} - \alpha_S)$. Assume (17) holds for all *t*, then

$$\begin{aligned} P_{t+1}^{(1)} &= (1-\alpha_{SL})P_t^{(1)} + (\alpha_{SL} - \alpha_S)P_{t-1}^{(1)} \\ &= (1-\alpha_{SL})(\alpha_{SL} - \alpha_S)P_{t-1}^{(2)} + (\alpha_{SL} - \alpha_S)^2 P_{t-2}^{(2)} \\ &= (\alpha_{SL} - \alpha_S)P_t^{(2)} \end{aligned} \tag{18}$$

We denote L_t as a region in which $P_t^{(2)} < 0$ and $P_{t-1}^{(2)} > 0$, and $P_t^{(2)} = 0$ gives the boundaries between them. Clearly in L_t we have $P_t^{(2)} < 0$ and $P_t^{(1)} < 0$ since $\alpha_{SL} - \alpha_S < 0$. Therefore $o_t \le P_t^{(0)}$ due to the non-negativity of orders. □

In general, $P_t^{(0)}$ gives the upper bound of order oscillation and $P_t^{(2)} = 0$ gives the boundaries. As *t* increases, $P_t^{(0)}$ takes different forms. We denote $o_{t,\mathrm{II}}^{\max} = P_t^{(0)}$, in which a subscript II is used to represent that this is the upper bound of orders in region II. Some expressions of upper bounds and boundaries in the first few periods are summarized in Table 1.

Table 1. Upper bounds and boundaries in region II

t	$o_{t,\mathrm{II}}^{\max} = P_t^{(0)}$	$P_t^{(2)} = 0$
3	α_S	$\alpha_{SL} = 1$
4	$-\alpha_S\alpha_{SL} + 2\alpha_S$	$\alpha_S = \alpha_{SL}^2 - \alpha_{SL} + 1$
5	$-\alpha_S^2 + (\alpha_{SL}^2 - 2\alpha_{SL} + 3)\alpha_S$	$\alpha_S = \frac{1}{2}(\alpha_{SL}^2 + 1)$
6	$(2\alpha_{SL} - 3)\alpha_S^2 - (\alpha_{SL}^3 - 2\alpha_{SL}^2 + 3\alpha_{SL} - 4)\alpha_S$	$\alpha_S = \frac{3}{2}\alpha_{SL}^2 - 2\alpha_{SL} - \frac{\sqrt{5}}{2}(\alpha_{SL} - 1)^2 + \frac{3}{2}$
7	$\begin{pmatrix} \alpha_S^3 - (3\alpha_{SL}^2 - 6\alpha_{SL} + 6)\alpha_S^2 + \\ (\alpha_{SL}^4 - 2\alpha_{SL}^3 + 3\alpha_{SL}^2 - 4\alpha_{SL} + 5)\alpha_S \end{pmatrix}$	$\alpha_S = \frac{1}{3}(\alpha_{SL}^2 + \alpha_{SL} + 1)$

According to (16), $P_t^{(0)}$ happens to be the solutions of the characteristic difference equation (12). Also notice that $P_t^{(0)} = 1 - \mathrm{tr}(\mathbf{A}_1^{t-2}\mathbf{A}_2)$. Moreover, $P_t^{(2)} = 0$ is equivalent to setting the following continued fraction to zero,

$$\underbrace{\mathrm{tr}(\mathbf{A}_1) - \cfrac{|\mathbf{A}_1|}{\mathrm{tr}(\mathbf{A}_1) - \cfrac{|\mathbf{A}_1|}{\mathrm{tr}(\mathbf{A}_1) - \cdots}}}_{t\text{-tuple continued fraction}} = 0. \tag{19}$$

Figure 7a gives an example of order oscillations in this region with $\alpha_S = 1$ and $\alpha_{SL} = -1.5$. We know from the previous analysis that the system is not stable. However, complex eigenvalues make the vibration slow, smooth and periodic-like. Large positive orders are separated by long intervals of zero orders.

The bifurcation map when $\alpha_S = 1$ is shown in Figure 7b. It is clearly seen that the upper bounds can only be expressed piecewise, and the bifurcation is enclosed by curves of $P_t^{(0)}$. When $\alpha_S = 1$, the upper bound expression changes at $\alpha_{SL} = -\frac{1+\sqrt{5}}{2}$, the golden ratio, and $\alpha_{SL} = -1$. Although all the curves are polynomial, the upper bound of the orders increases to infinity as $\{\alpha_S, \alpha_{SL}\}$ approaches the boundary of divergence.

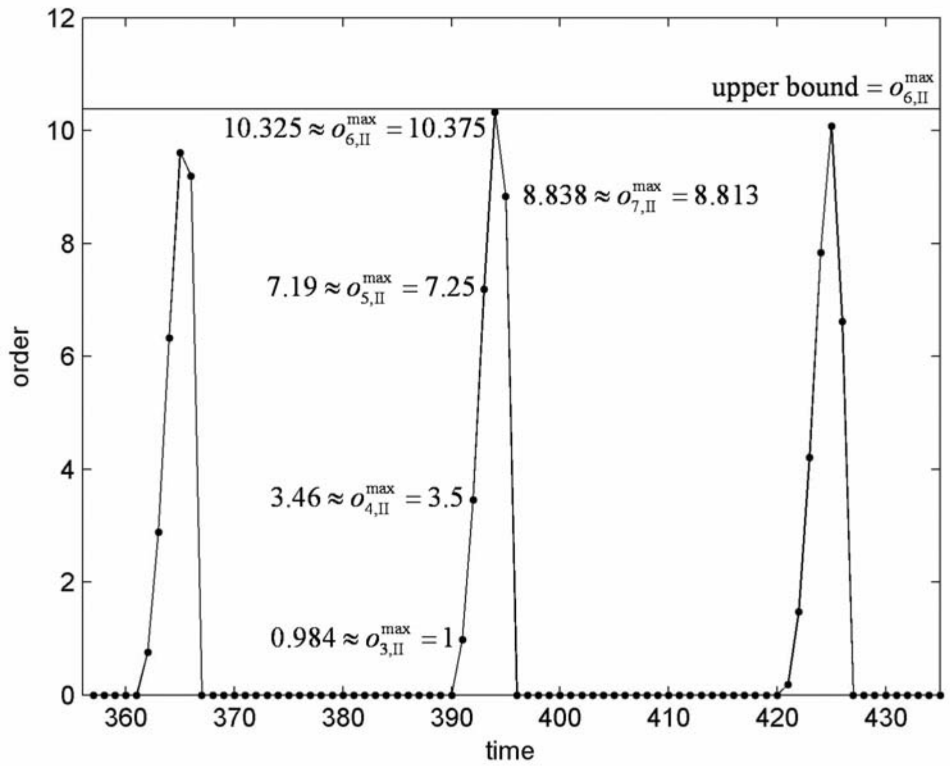

(a) Time-series plot. $\alpha_S = 1$, $\alpha_{SL} = -1.5$.

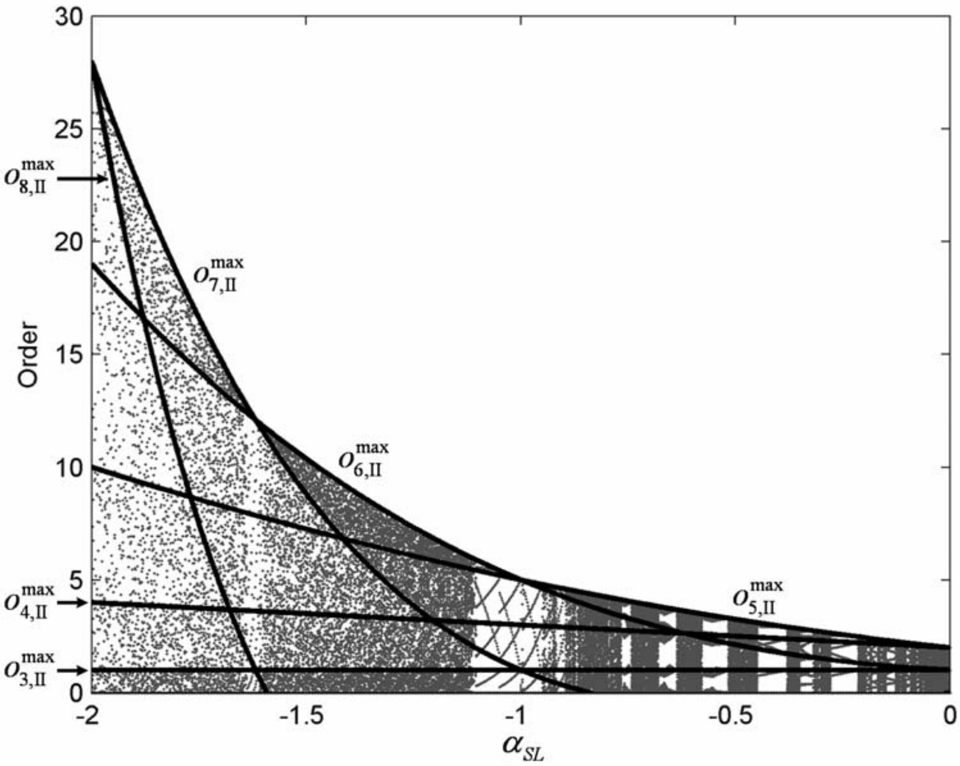

(b) Bifurcation diagram, $\alpha_S = 1$.

Figure 7. Time series plot and bifurcation diagram of typical order oscillations in region II, $\alpha_S = 1$.

Inventory systems with parameters in region III oscillate in a more chaotic pattern. Systems in this area are dominated by one negative real eigenvalue outside the unit circle and one positive real eigenvalue inside the unit circle, and fluctuate at a much higher frequency than systems with complex eigenvalues. In this area, instead of precise upper bounds, we have discovered that the bifurcation maps are stratified. The curves we are able to derive are no longer the upper bound of order oscillation. Instead, they divide the bifurcation into several layers (sections) in which the order volume has a different probability density. Here one can only claim with a certain probability that the order volume is smaller than one of these curves. Through time series speculation (Figure 8a) we have observed the following fact which may help explain the stratifying effect in this region: a large order often follows a small fluctuation. The longer the small fluctuation lasts for, the larger the order will be which is less likely to happen. This can be verified by the following analysis. Starting from t = 3, we make certain transformations from (12) to obtain the form

$$o_t = Q_t^{(2)} o_{t-1} + Q_t^{(1)} o_1 + Q_t^{(0)} , \tag{20}$$

$t \in \mathbb{N}^+$, $t \geq 3$ .The following iterative relationships can then be found by induction,

$$Q_t^{(2)} = 1 - \alpha_{SL} + \frac{\alpha_{SL} - \alpha_S}{Q_{t-1}^{(2)}} , \tag{21}$$

$$Q_t^{(1)} = -\frac{(\alpha_{SL} - \alpha_S) Q_{t-1}^{(1)}}{Q_{t-1}^{(2)}} , \tag{22}$$

$$Q_t^{(0)} = -\frac{(\alpha_{SL} - \alpha_S) Q_{t-1}^{(0)}}{Q_{t-1}^{(2)}} + \alpha_S . \tag{23}$$

Since $1 - \alpha_{SL} < 0$, $\alpha_{SL} - \alpha_S > 0$ in region III, $Q_t^{(2)}$ is guaranteed to be negative and $Q_t^{(1)}$ is always positive. We use $o_{t,\mathrm{III}}^{\max} = Q_t^{(0)}$ to denote the approximate upper bound in region III. By simple observation we have find that $\lim_{\alpha_{SL}\to+\infty} o_{t,\mathrm{III}}^{\max} = (t-2)\alpha_S$. Another important limit is

$$\lim_{t\to\infty} o_{t,\mathrm{III}}^{\max} = o_{\infty,\mathrm{III}}^{\max} = \frac{1+\alpha_{SL}+\sqrt{(1+\alpha_{SL})^2-4\alpha_S}}{2} \tag{24}$$

which gives us the absolute boundary of the maximum possible order quantity. This is derived by computing the final values of $Q_t^{(2)}$ and $Q_t^{(0)}$ from (21) and (23). When $\alpha_{SL}\to\infty$, (24) approaches $\alpha_{SL}+1$, independent of α_S.

We have listed several stratifying curves below and drawn them along with the bifurcation map in Figure 8b. For the sake of clarity the range of α_{SL} is extended. We can see that the stratifying curves fit very well with the bifurcation map.

Table 2. Approximate upper bounds in region III

t	$o_{t,\mathrm{III}}^{\max} = Q_t^{(0)}$
3	α_S
4	$-\frac{\alpha_S(\alpha_{SL}-\alpha_S)}{1-\alpha_{SL}}+\alpha_S$
5	$\frac{\alpha_S(\alpha_{SL}-\alpha_S)(2\alpha_{SL}-\alpha_S-1)}{\alpha_{SL}^2-\alpha_{SL}-\alpha_S+1}+\alpha_S$
6	$\frac{\alpha_S(\alpha_{SL}-\alpha_S)(-\alpha_S^2+2\alpha_{SL}-3\alpha_{SL}^2+3\alpha_S\alpha_{SL}-1)}{(1-\alpha_{SL})(1-2\alpha_S+\alpha_{SL}^2)}+\alpha_S$
7	$\frac{\alpha_S(\alpha_{SL}-\alpha_S)\left[-1+\alpha_S-\alpha_S^3+2(1+2\alpha_S^2)\alpha_{SL}-3(1+2\alpha_S)\alpha_{SL}^2+4\alpha_{SL}^3\right]}{1-3\alpha_S+\alpha_S^2+(4\alpha_S-1)\alpha_{SL}+(1-3\alpha_S)\alpha_{SL}^2-\alpha_{SL}^3+\alpha_{SL}^4}+\alpha_S$

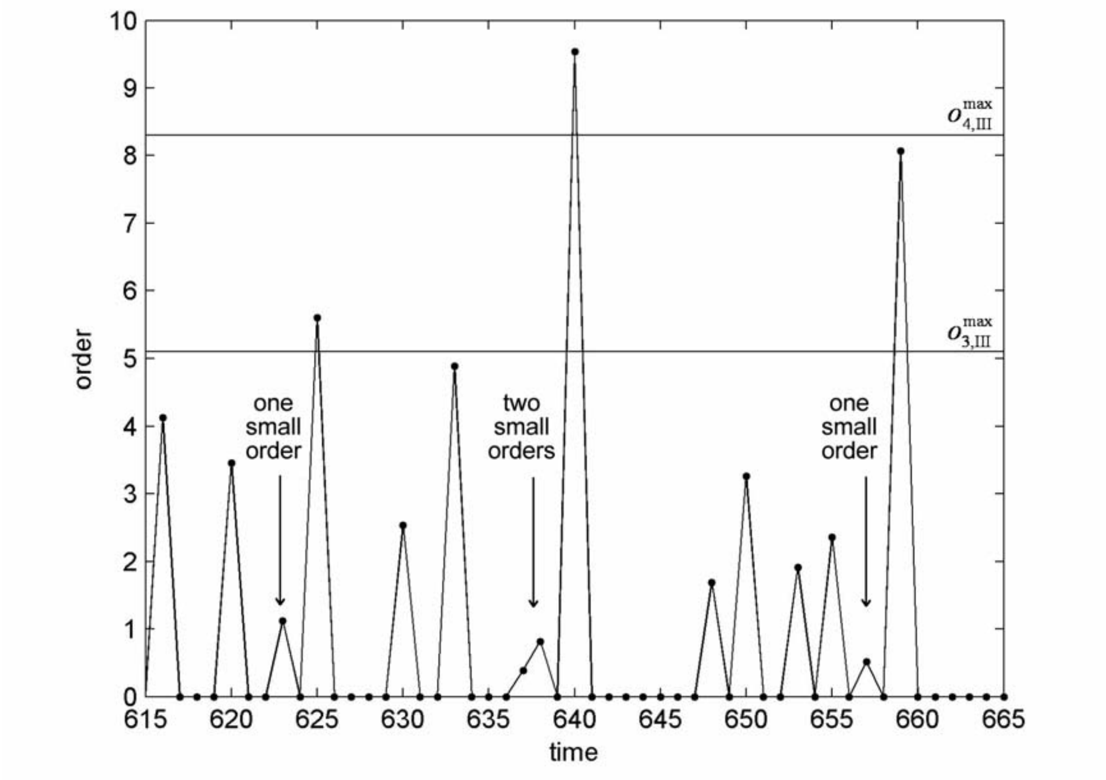

(a) Time-series plot, $\alpha_S = 5.1$, $\alpha_{SL} = 12$.

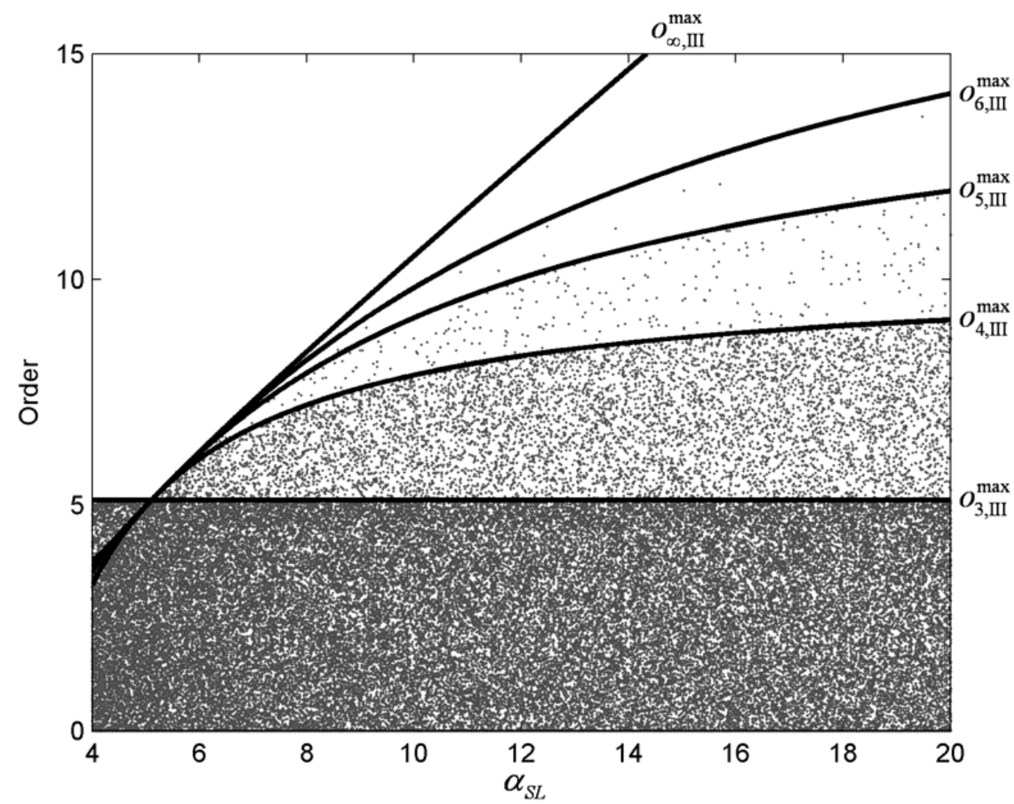

(b) Bifurcation diagram, $\alpha_S = 5.1$.

Figure 8. Time series plot and bifurcation diagram of typical order oscillations in region III, $\alpha_S = 5.1$.

It is found that the parameter settings adjacent to the convergence region generate small oscillations. On the contrary, remote parameter settings, no matter in which direction, will increase the mean and amplitude of the oscillation. Only the velocity of such increases will vary. For instance, starting from the convergence area, increasing α_{SL} is expected to generate a linear growth in the maximum order oscillation, and decreasing a negative α_{SL} will generate an almost exponential growth.

4.2 Oscillations in the inventory

The upper and lower bound of inventory oscillation can also be calculated by investigating its dynamics. In the period 2 region, the inventory fluctuation follows

$$\cdots \ \frac{\alpha_{SL}-1}{\alpha_S}, \ \frac{\alpha_S+\alpha_{SL}-1}{\alpha_S}, \ \frac{\alpha_{SL}-1}{\alpha_S}, \ \frac{\alpha_S+\alpha_{SL}-1}{\alpha_S}, \ \frac{\alpha_{SL}-1}{\alpha_S}, \ \frac{\alpha_S+\alpha_{SL}-1}{\alpha_S}, \ \cdots \tag{25}$$

In Region I and II, we notice that the minimum inventory level (denoted $i_{\mathrm{I,II}}^{\min}$) always appears one period after the first order, because this order will be received and inventory level will rise one period after the minimum inventory level. Remember also that before the first order the system is in a full consumption state without compensation. Consequently, the inventory level one period before $i_{\mathrm{I,II}}^{\min}$ generates an order of α_S, which means that

$$(1+\alpha_S+\alpha_{SL})-\alpha_S(i_{\mathrm{I,II}}^{\min}+1)=\alpha_S\ . \tag{26}$$

Rearranging we have

$$i_{\mathrm{I,II}}^{\min}=\frac{\alpha_{SL}-\alpha_S+1}{\alpha_S}\ . \tag{27}$$

Likewise, the maximum inventory level ($i_{t,\mathrm{I,II}}^{\max}$) appears two periods after the last order in a cycle, which is its completion time. It is equal to the minimum inventory level plus the sum of orders less the sum of the consumption in the cycle:

$$i_{t,\mathrm{I,II}}^{\max}=i_{\mathrm{I,II}}^{\min}+\sum_{j=1}^{t}o_{j,\mathrm{I,II}}^{\max}-t=\sum_{j=1}^{t}o_{j,\mathrm{I,II}}^{\max}+\frac{\alpha_{SL}-\alpha_S+1}{\alpha_S}-t\ . \tag{28}$$

In region III, there are both upper and lower stratifying curves. Notice that the minimum inventory appears one period after the maximum order rate, and maximum inventory appears two periods after the maximum order rate. Using similar methods, the approximate bounds in region III can be derived as:

$$i_{t,\mathrm{III}}^{\min}=\frac{1+\alpha_{SL}-o_{t,\mathrm{III}}^{\max}}{\alpha_S} \tag{29}$$

$$i_{t,\mathrm{III}}^{\max}=\frac{(\alpha_S-1)o_{t,\mathrm{III}}^{\max}+\alpha_{SL}-\alpha_S+1}{\alpha_S}\ . \tag{30}$$

The upper and lower bound of the inventory oscillation are both increasing in α_{SL} and decreasing in α_S.

5. Conclusions and managerial implications

We have highlighted the range of dynamic behaviours that are present in a constrained inventory system with only one constraint, forbidden returns. The stable region of the forbidden return system is identical to that of the linear system, indicating that existing knowledge and methodologies for studying the asymptotic stability of linear inventory systems can be applied to the forbidden returns case. We have shown that a complex and diversified set of behaviours and patterns exist outside the convergence region. When operating outside the convergence region, the inventory system may not escape to infinity as would be inferred by a linear analysis; the risk of catastrophic divergence is reduced by the physical constraint. Divergence only appears when there is a positive feedback on inventory or strong positive feedback on WIP. In other cases, if there is an oscillation, the oscillation will be bounded. Under certain parameter settings, the oscillation will show a periodic pattern, most noticeably when WIP feedback gain is larger than the inventory feedback gain. It is reasonable to conjecture that when facing a stochastic demand, system behaviour will be more predictable when the parameters are in this region. Moreover, we found it interesting that even a simple deterministic model with a short, known and constant lead-time is sufficient to generate such complex phenomena. We wonder what sort of impact stochastic demand, longer or random lead-times and more constraints will have?

Through a numerical experiment, we have shown the Bullwhip Effect in a nonlinear inventory system is largely affected by the intrinsic oscillations produced by the system. Therefore it is essential, as a first step, to study the deterministic oscillation amplitude of the inventory system with respect to both order and inventory. We have demonstrated how to determine the type and bound of each oscillation. It is found that whilst system stability is determined by the modulus of eigenvalues, the oscillation amplitude is governed by their real parts. The upper bound of the oscillations can be expressed piecewise by solutions of the dominating difference equation, and the amplitude of order and inventory oscillations will be smaller if control parameters are set closer to the stable region. For period-2 oscillation, the amplitude of both order and inventory is constant. In the region $1 < \alpha_{SL} < \alpha_S$ the oscillation of order is constrained to below α_S. As can be predicted, setting parameters close to the divergence boundary will create massive order quantities, but with very long intervals between orders. As would be expected there is also a tendency that large orders are followed by long intervals of zero orders. This approach may be suitable in situations when there is a significant order set-up cost and it may be useful to compare performance to the Economic Order Quantity model.

The lead-time of the inventory system is limited to one period in this paper, where the conventional settings, $0 < \{\alpha_S, \alpha_{SL}\} \le 1$, are guaranteed to be stable. However when the lead-time increases this is not the case. Settings with a large inventory gain and small WIP gain are the most vulnerable to a lead-time increase in terms of stability. Nonlinear oscillations in such scenarios can then be analyzed using a similar approach. Moreover, there is a possibility that supply chain participants will use an intuitive ordering policy rather than a carefully designed one. In this case decision makers are more likely to move the parameters out of the stability area. Therefore an expansion of the control plane provides a more thorough understanding of the dynamic nature of a constrained inventory system.

Potential future research could involve several aspects. One is to incorporate other constraints, such as lost sales and forbidden outsourcing, into the inventory system model. Our own preliminary investigation has shown that when lost sales are solely present, the stable region will be sensitive to the initial values of the inventory and orders. Another idea for future work is to expand our study of the oscillation when the system is exposed to random external disturbances. The intrinsic oscillation would then be coupled with random noise. Yet another avenue of investigation could be to study how different types of oscillation evolve along a multi-echelon supply chain, i.e., the so-called 'chaos-amplification' effect, as a nonlinear counterpart to the linear 'variance amplification' (or bullwhip) effect.

Acknowledgments

This research is partially supported by Chinese National Foundation of Natural Science (No.70872009; No.70821061; No.71172016). X. Wang would like to thank Chinese Scholarship Council for providing financial support (No. 2010602068) for a one-year academic visit to Cardiff University. We would also like to thank the anonymous referees for their invaluable help and suggestions.

References

Åström, K.J., 1970. Introduction to stochastic control theory. Academic Press, New York.

Aviv, Y., 2003. A time-series framework for supply-chain inventory management. Operations Research, 51(2), 210-227.

Chen, F., Drezner, Z., Ryan, J., Simchi-Levi, D., 2000. Quantifying the bullwhip effect in a simple supply chain: The impact of forecasting, lead times, and information. Management Science, 46(3), 436–443.

Dai, L., Han, L., 2011. Analyzing periodicity, nonlinearity and transitional characteristics of nonlinear dynamic systems with Periodicity Ratio (PR). Communications in Nonlinear Science and Numerical Simulation, 16(12), 4731-4744.

Dejonckheere J., Disney, S.M., Lambrecht, M.R., Towill, D.R., 2004. The impact of information enrichment on the bullwhip effect in supply chains: A control engineering perspective. European Journal of Operations Research, 153(3), 727-750.

Dejonckheere, J., Disney, S.M., Lambrecht, M.R., Towill, D.R., 2003. Measuring and avoiding the bullwhip effect: A control theoretic approach. European Journal of Operational Research, 147(3), 567–590.

di Bernardo, M., Feigin, M.I., Hogan, S.J., Homer M.E., 1999. Local Analysis of C-bifurcations in n-dimensional piecewise-smooth dynamical systems. Chaos, Solitons & Fractals, 10(11), 1881-1908.

Disney, S.M., 2008. Supply chain aperiodicity, bullwhip and stability analysis with Jury's Inners. IMA Journal of Management Mathematics, 19(2), 101-116.

Disney, S.M., Towill, D.R., 2003a. The effect of Vendor Managed Inventory (VMI) on the bullwhip effect in supply chains. International Journal of Production Economics, 85(2), 199-215.

Disney, S.M., Towill, D.R., 2003b. On the bullwhip and inventory variance produced by an ordering policy. Omega: The International Journal of Management Science, 31(3), 157-167.

Gaalman, G., 2006. Bullwhip reduction for ARMA demand: The proportional order-up-to policy versus the full-state-feedback policy. Automatica, 42(8), 1283-1290.

Galias, Z., Ogorzalek, M.J., 1990. Bifurcation phenomena in second-order digital filter with saturation-type adder overflow characteristic. IEEE Transactions on Circuits and Systems, 37(8), 1068-1070.

Geary, S., Disney, S.M., Towill, D.R., 2006. On bullwhip in the supply chains ~ historical review, present practice and expected likely impact. International Journal of Production Economics, 101(1), 2-18.

Hosoda, T., Disney, S.M., 2009. Impact of market demand mis-specification on a two-level supply chain. International Journal of Production Economics, 121(2), 739-751.

Hosoda, T., Disney, S.M., 2012. A delayed demand supply chain: incentives for upstream players. Omega, 40(4), 478-487.

Hwarng, H.B., Xie, N., 2008. Understanding supply chain dynamics: a chaos perspective. European Journal of Operational Research, 184(3), 1163-1178.

Laugesen, J., Mosekilde, E., 2006. Border-collision bifurcations in a dynamic management game. Computers & Operations Research, 33(2), 464-478.

Lee, H.L., Padmanabhan, V., Whang, S., 1997. Information distortion in a supply chain: The bullwhip effect. Management Science, 43(4), 546–558.

Lee, H.L., So, K.C., Tang, C.S., 2000. The value of information sharing in a two-level supply chain. Management Science. 46(5), 626-643.

Liu, H., 2005. Research on dynamics of supply chain, Ph.D. Dissertation, Huazhong University of Science and Technology, P.R. China.

Martichenko, R., von Grabe, K., 2010. Building a lean fulfillment stream, Lean Enterprise Institute, Cambridge, USA.

Mosekilde, E., Larsen, E.R., 1988. Deterministic chaos in the beer production distribution model. System Dynamics Review, 4(1), 131-147.

Mosekilde, E., Laugesen J.L., 2007. Non-linear dynamic phenomena in the beer model. System Dynamics Review, 23, 229-252.

Nagatani, T., Helbing, D., 2004. Stability analysis and stabilization strategies for linear supply chains, Physica A, 335(3-4), 644-660.

Ogorzalek, M.J., Galias, Z, 1991. Arnold tongues and devil's staircase in a digital filter employing saturation arithmetic. IEEE International Symposium on Circuits and Systems, Singapore.

Rodrigues, L., Boukas, E., 2006. Piecewise-linear H∞ controller synthesis with applications to inventory control of switched production systems. Automatica, 42(8), 1245-1254.

Sarimveis, H., Patrinos, P., Tarantilis, C.D., Kiranoudis, C.T., 2008. Dynamic modeling and control of supply chain systems: A review. Computers & Operations Research, 35(11), 3530-3561.

Sterman, J.D., 1989. Modelling managerial behavior: Misperceptions of feedback in a dynamic decision making experiment. Management Science, 35(3), 321-339.

Sun, Z., 2010. Stability of piecewise linear systems revisited. Annual Reviews in Control, 34(2), 221-231.

Thompson, J.M.T., Stewart, H.B., 1986. Nonlinear Dynamics and Chaos. Wiley, New York.

Thomsen, J.S., Mosekilde, E., Sterman, J.D., 1992. Hyperchaotic phenomena in dynamic decision making. System Analysis and Modelling Simulation, 9, 137-156.

Towill, D.R., Disney, S.M., 2008. Managing bullwhip induced risks in supply chains. International Journal of Risk Assessment and Management, 10(3), 238-262.

Wang, K.J., Wee, H.M., Gao, S.F., Chung, S.L., 2005. Production and inventory control with chaotic demands. Omega: The International Journal of Management Science, 33(2), 97-106.

Wu, Y., Zhang, D.Z., 2007. Demand fluctuation and chaotic behaviour by interaction between customers and suppliers. International Journal of Production Economics, 107(1), 250-259.

Zhusubaliyev, Z.T., Mosekilde, E., 2003. Bifurcations and chaos in piecewise-smooth dynamical systems. World Scientific, Singapore

Research highlights

- We model an inventory system where return of goods is not allowed.

- Criteria for stability and periodicity of the constrained inventory system are identified.
- Analytical upper bounds of the order and inventory oscillations are derived.
- Parameter settings that lead to different classes of dynamic behaviour are identified.